Oxygen-Vacancy-Induced Diffusive Scattering in Fe/MgO/Fe Magnetic Tunnel Junctions

Youqi Ke,[1] Ke Xia,[2] and Hong Guo[1]

[1]*Centre for the Physics of Materials and Department of Physics, McGill University, Montreal, PQ, H3A 2T8, Canada*
[2]*Department of Physics, Beijing Normal University, Beijing 100875, China*

(Received 12 August 2010; revised manuscript received 3 October 2010; published 30 November 2010)

By first principles analysis, we systematically investigate effects of oxygen vacancies (OV) in the MgO barrier of Fe/MgO/Fe magnetic tunnel junctions. The interchannel diffusive scattering by disordered OVs located at or near the Fe/MgO interface drastically reduces the tunnel magnetoresistance ratio (TMR) from the ideal theoretical limit to the presently observed much smaller experimental range. Interior OVs are far less important in influencing TMR, but they significantly increase the junction resistance. Filling OV with nitrogen atoms restores TMR to near the ideal theoretical limit.

DOI: 10.1103/PhysRevLett.105.236801 PACS numbers: 85.35.−p, 72.25.Mk, 73.63.Rt, 75.47.De

One of the most important spintronics phenomena [1] is the tunnel magnetoresistance (TMR) observed in magnetic tunnel junctions (MTJ). MTJ is made of two ferromagnetic layers sandwiching a thin insulating tunnel barrier. The tunneling current $I_{\uparrow\uparrow}$ is large when magnetic moments of the two ferromagnetic layers are in parallel configuration (PC or $\uparrow\uparrow$) and $I_{\uparrow\downarrow}$ is small when they are antiparallel (APC or $\uparrow\downarrow$). The larger the TMR ratio, $(I_{\uparrow\uparrow} - I_{\uparrow\downarrow})/I_{\uparrow\downarrow}$, the more sensitive the device. MTJ is the fundamental device element for practical systems such as read sensors and magnetic random access memory. In 2004, experiments [2,3] achieved large TMR ratio ~200% in MgO based MTJ using CoFe or Fe as electrodes. Since then, improvement of materials increased TMR to slightly larger than 1100% at low temperatures [4]. On the other hand, for ideal Fe/MgO/Fe MTJ, first principles theoretical calculations predicted much higher TMR ratio [5,6], up to 10 000%. A very important problem is to identify and therefore rectify detrimental effects that prevent experimental TMR ratio from reaching much higher values.

For ideal clean Fe/MgO/Fe junctions, as explained clearly before [5], by symmetry the minority-spin d states having transverse momentum $k_{\|} \neq (0, 0)$ in Fe cannot couple to the slowly decaying Δ_1 band of MgO at $k_{\|} = (0, 0)$. These Fe states are therefore filtered out by MgO. Furthermore, the majority-spin channel in the left Fe cannot tunnel through in APC because the right Fe is in the antiparallel state. The overall result is a very small APC current and a large spin polarized PC current, giving rise to the huge TMR in the ideal limit.

It is therefore generally believed that atomic defects in the experimental MTJ is the likely cause for not reaching the ideal theoretical TMR limit because defect scattering can destroy the tunneling symmetry. One such effect [7–9] is the possibility of extra oxygen atoms at the Fe/MgO interface forming a FeO layer. On the other hand, experiments on devices with clean, nonoxidized Fe/MgO interfaces [10] still report a TMR ratio far from the theoretical ideal limit. Calculations showed that small Fe/MgO interface structural randomness also drops TMR [8], but not enough to reach the current experimental range. More recently, experiments were carried out to investigate another kind of defects, oxygen vacancies (OV) inside the MgO barrier [11], and Ref. [12] provided direct experimental evidence of localized defect states inside the MgO energy gap which was attributed to the OV. Theoretical investigation of OV effects on TMR is rather limited. Reference [13] reported a supercell density functional theory (DFT) calculation in which one oxygen atom in MgO was removed; this defect reduced the TMR ratio from the ideal limit by a factor of roughly 2.

Oxygen vacancy in MgO is quite likely due to a compressive strain at the Fe/MgO interface during crystal growth [12]. Here we report a systematic first principles analysis of its effect. By placing OVs at interfacial layers or interior layers in the MgO, a general trend is discovered: (i) merely a few percent of OV at or near the Fe/MgO interface drops the TMR ratio from ~10 000% to the experimental range due to an efficient reduction of specular scattering in favor of diffusive scattering that causes the minority-spin channel in Fe to scatter into the Δ_1 band of MgO; (ii) effects of interior OV on TMR are far less important, they however break the Δ_1 wave function symmetry of MgO thereby significantly increase the junction resistance; (iii) filling OV with nitrogen atoms, the ideal TMR limit is partially recovered.

Our calculation is based on DFT within the Keldysh nonequilibrium Green's function (NEGF) formalism [14]. The disorder averaging of results is carried out by the theory of nonequilibrium vertex corrections (NVC) [15]. Briefly, for systems without disorder, NEGF DFT [14] calculates density matrix by NEGF as $\rho \sim \int dE\mathbf{G}^{<}$, and transmission coefficient as $T = \mathrm{Tr}[\mathbf{G}^{\mathbf{r}}\Gamma_L\mathbf{G}^{\mathbf{a}}\Gamma_R]$, where $\mathbf{G}^{\mathbf{r,a},<}$ are the retarded, advanced, and lesser Green's functions, respectively, and $\mathbf{\Gamma_{L,R}}$ are the line width functions of the left (L) and right (R) leads. For disordered systems, the configuration average is carried out by NVC such that [15]:

$$\bar{\rho} \sim \int dE\bar{\mathbf{G}}^{<} \equiv \int dE\bar{\mathbf{G}}^{r}(\mathbf{\Sigma}^{<} + \mathbf{\Omega}_{\mathrm{NVC}})\bar{\mathbf{G}}^{a}, \quad (1)$$

$$\bar{T} = \mathrm{Tr}[\overline{\mathbf{G}^{r}\Gamma_{L}\mathbf{G}^{a}\Gamma_{R}}] = \mathrm{Tr}[\bar{\mathbf{G}}^{r}\Gamma_{L}\bar{\mathbf{G}}^{a}\Gamma_{R}] + \mathrm{Tr}[\bar{\mathbf{G}}^{r}\Gamma_{L}\bar{\mathbf{G}}^{a}\Omega'_{\mathrm{VC}}]. \quad (2)$$

Here $\Sigma^{<} = i(\Gamma_L f_L + \Gamma_R f_R)$ is the lesser self-energy due to the device leads and $f_{L,R}$ are their Fermi functions. The configuration average, indicated by $\overline{(\cdots)}$, correlates the forward and backward propagators $\mathbf{G}^r$ and $\mathbf{G}^a$: the correlation accounts for the multiple electron scattering due to impurities. Mathematically, the disorder averaging is facilitated by a NVC self-energy Ω_{NVC} at the nonequilibrium density matrix level, and by an additional equilibrium vertex term Ω'_{VC} at the transmission coefficient level. The NEGF-DFT-NVC formalism is implemented within the linear muffin tin orbital first principle framework [15–17]. The exchange correlation is treated by local spin density approximation. Coherent potential approximation [18] is applied to calculate configuration averages of $\bar{\mathbf{G}}^{r,a}$. Finally, in the transmission coefficient Eq. (2), the first term on the right-hand side accounts for specular scattering and the second term—vertex correction—accounts for diffusive scattering. The conductance is $\bar{T}(e^2/h)$, where e is the electron charge and h the Planck constant.

Figure 1 shows the Fe/MgO/Fe atomic structure in our analysis [19]. A vacancy is created by randomly replacing an oxygen atom with a vacuum sphere (Va) of the same size, where a small structural distortion is neglected [20]. The substitutional disorder is realized by the alloy model $O_{1-x}Va_x$ where percentage x is an input parameter. We first calculated [21] perfect junctions (no OV) having $L = 3$–13 monolayers of MgO. Conductances of all spin channels decay exponentially versus L as expected from tunneling. TMR ratio increases rapidly with L, reaching ~10 000% for the 13-layer MgO device. A perfect junction gives purely specular tunneling which conserves transverse momentum $k_{\|}$, and its conductance in PC is dominated by the spin-up channel. These results are consistent with previous work [5,6,8]. For junctions with OV, we shall focus on the 13-layer MgO which was studied experimentally [11]. Putting OVs at different MgO layers [22] (Fig. 1), a clear trend emerges.

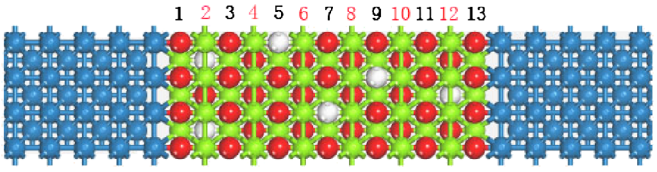

FIG. 1 (color online). Atomic structure of Fe/MgO/Fe junction with a 13-layer MgO barrier. Blue spheres, Fe; red spheres, O; green spheres, Mg; white spheres, oxygen vacancy. The junction is periodically extended in the transverse directions. The numbers label MgO layers from the left to the right.

Interfacial OV.—Fixing 3% OV on layer 1 of the MgO and x% on layer 13, leaving the rest of the MgO layers perfect, the results are shown in Fig. 2. Figures 2(a) and 2(b) plot conductance versus x for PC and APC. The most striking result is that the vertex correction in transmission, e.g., the second term of Eq. (2), plays a dominant role in all spin channels. As Figs. 2(a) and 2(b) show, the spin-down channel in PC and all channels in APC are almost entirely contributed by diffusive scattering. The OVs assist minority-spin channels in Fe to traverse the MTJ by introducing interchannel scattering which couples these states to the slowly decaying Δ_1 band of the MgO. As a result the coherent spin filtering effect [5] is drastically reduced. The conductance in APC increases significantly, resulting in a drastic reduction of the TMR ratio. Shown in Fig. 2(c), for several OV distributions, TMR reduces dramatically from the ideal limit of ~10 000% to ~250% when x is merely 4%. To emphasize the dominating role of interfacial OV, on top of 3% OV in layers 1 and 13, we add a further x% in layer 7. As the inset of Fig. 2(d) shows, the TMR stays at ~350% almost independent of the layer 7 x.

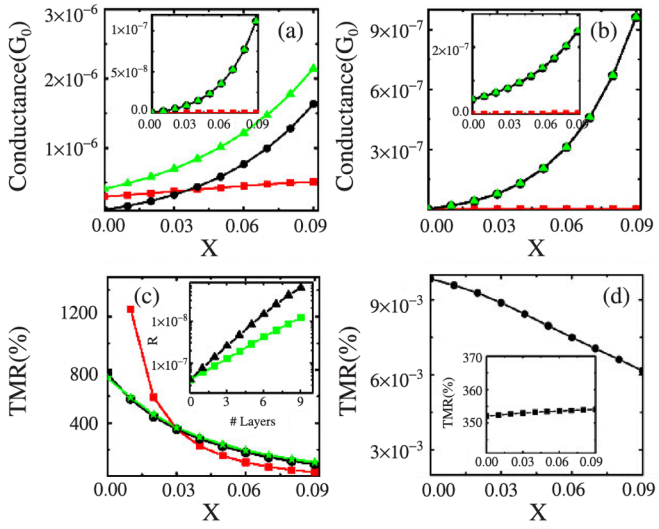

FIG. 2 (color online). (a),(b) Conductance versus OV concentration x at equilibrium for spin-up and -down (insets) channels in PC (a) and AP (b). Layer 1 of MgO is fixed with 3% OV; layer 13 with x%. Green up-triangles, total conductance; red squares, coherent part; black circles, vertex correction part. (c) TMR versus x for several MTJs. Red squares, for symmetric junctions with x% OV at both layers 1 and 13. Black circles, for asymmetric junctions with 3% OV on layer 1 and x% on layer 13. Green stars, same disorder distribution as the black circles but for a junction having 7-layer MgO barrier. Inset: Log-10 scaled resistance versus number of disordered MgO layers (3, 3–43–4–5, 3–4–5–6, ...) for spin-up channel in PC: green squares are for 3% OV; black up-triangles for 5%. (d) TMR versus x for a 13-layer junction where interfacial OVs are filled by nitrogen atoms; namely, x% nitrogen atoms replace oxygen atoms on the 1st and 13th MgO layer. Inset: TMR versus x for a junction with 3% OV on both layer 1 and layer 13, at the same time x% OV on layer 7.

Next-neighbor OV.—When the OVs are located at layers 2 and 12, and all other MgO layers are clean, the effects are found to be qualitatively the same as that of the interfacial OV. Again, the TMR is diminished very quickly from the theoretical ideal limit to ~250% when OV concentration x is less than a few percent [similar to Fig. 2(c)]. With 3% OV on layers 2 and 12, adding further OVs in the middle layers of MgO does not significantly reduce TMR indicating, again, the importance of OVs near the Fe/MgO interface. We have calculated junctions with both interfacial OV and next-neighbor OV, the TMR drops more quickly. The only main difference between the interfacial OV and the next-neighbor OV is the behavior of PC conductance. For the interfacial OV, Fig. 2(a) shows an increasing conductance versus x; for the next-neighbor OV, it is a decreasing conductance. For APC the conductance behaves the same as that of Fig. 2(b). An interfacial OV layer in effect reduces the width of the perfect MgO tunnel barrier, thus enhancing the tunneling probability. On the other hand, OVs (especially the interior OVs) provide scattering centers that reduce tunneling.

Interior OV and interface roughness.—Leaving the interfacial and next-neighbor MgO layers clean, a few percent interior OVs can reduce TMR but much less drastically. For example, when 5% OVs are put on layer 3, we found that the total APC conductance is almost the same as the perfect junction while the PC spin-up transmission is decreased by roughly 2; TMR is reduced from ~10 000% to 4067%. Putting OV in layer 7 while keeping all other layers clean, TMR is only reduced to 7727% even when $x = 9\%$. By systematically putting the same concentration of OV one layer at a time, the results show that the further away from the interface, the less effective it is for OV to quench TMR. Interior OV has less effect because the spin-down wave in Fe has more difficulty reaching them to cause interchannel scattering. In all interior OV (layers 3 to 11) configurations, the PC spin-up conductance $G_{P\uparrow}$ is found to decrease for increasing OV concentrations. For a comparison, we have investigated surface roughness scattering by replacing randomly Fe atoms at both Fe/MgO interfaces with $x\%$ of vacuum spheres ($Fe_{1-x}Va_x$). TMR is reduced steadily as x increases, reaching 2300% at $x = 9\%$. Hence, interface roughness is less effective than interfacial OV in reducing the TMR.

Junction resistance.—Experimentally, introducing OV to MgO layers can cause junction resistance to increase by 50 times [11]. The calculated resistance $1/G_{P\uparrow}$ as a function of disordered layers of MgO is shown in the inset of Fig. 2(c). Ten junctions with $x = 5\%$ (up-pointing triangles) and $x = 3\%$ (squares) OVs existing on layers 3, or on 3–4, or 3–4–5, . . . , or 3–4– . . . –10–11, are calculated. The resistances exhibit an exponentially fast increase: 5% OV causes 220-fold increase while 3% OV causes a 50-fold increase, consistent with experiment observation [11].

Transmission hot spots.—A general trend therefore emerges: small amount of OVs at or near the Fe/MgO interface efficiently turn specular scattering into diffusive scattering, causing spin-down minority channels in Fe to couple to the slowly decaying Δ_1 band of MgO, leading to dramatic reductions of the TMR ratio. This trend is vividly depicted in Fig. 3 which plots the $k_\parallel \equiv (k_x, k_y)$ resolved (hot spot) specular and vertex correction parts of the transmission coefficient, i.e., 1st and 2nd term of Eq. (2), for a symmetric junction having $x = 3\%$ OV at layers 1 and 13. In the specular part, all spin channels tunnel through the MgO barrier by conserving $k_\parallel$ and is largely concentrated around the Γ point $k_\parallel = 0$. The PC spin-up channel [Fig. 3(a)] is circular in $k_\parallel$ surrounding the Γ point, while the PC spin-down and the APC channels have a fourfold symmetry [Figs. 3(b), 3(e), and 3(f)]. From Fig. 3, the vertex part is spread much wider into the Brillouin zone (BZ) due to diffusive scattering and, most importantly, the APC spin-up vertex part [Fig. 3(g)] has a circular symmetry surrounding the Γ point which matches the symmetry of the Δ_1 band of MgO. As a result, the APC spin-up diffusive channel can easily pass through MgO via its Δ_1 band which increases APC current and reduces TMR. In APC, the specular part of spin-up and -down channels precisely equal each other [Figs. 3(e) and 3(f)] for all $k_\parallel$ due to the left or right atomic symmetry of this junction. The diffusive parts, Figs. 3(g) and 3(h), show completely different hot spots, but their total value after integrating the entire BZ are exactly the same. This is because the specular part conserves $k_\parallel$ while the diffusive part does not.

Bias dependence.—Figures 4(a) and 4(b) plot the calculated TMR versus bias voltage for a 7-layer MgO junction. For both clean and disordered interfacial layers the external bias reduces TMR even though the vertical scales of Figs. 4(a) and 4(b) are very different. TMR of the perfect

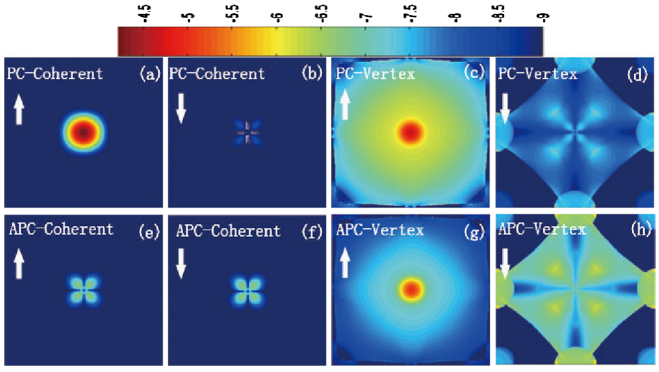

FIG. 3 (color online). $k_\parallel$ resolved transmission coefficient $T = T(E_f, k_x, k_y)$ in two-dimensional BZ for coherent and vertex parts of the spin-up and -down channels in PC and APC, for a junction with 3% OV on both layers 1 and 13. Here E_f is the Fermi energy of the Fe electrodes. (a)–(d) PC, (e),(f) APC. (a), (c),(e),(g) Spin-up channel, (b),(d),(f),(h) spin-down channel. (a),(b),(e),(f) Coherent part [1st term of Eq. (2)], (c),(d),(g), (h) vertex correction part [2nd term of Eq. (2)].

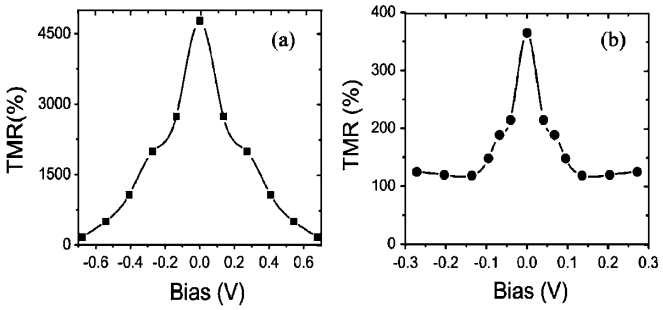

FIG. 4. TMR versus bias voltage for a 7-layer Fe/MgO/Fe MTJ. (a) Perfect junction without OV. (b) Junction with 3% OV on the interfacial layers 1 and 7 MgO.

junction drops to zero by the voltage, but it appears to saturate for the OV junction after the initial sharp drop. Experimentally, so far both fast drop [2,3] and much slower drop [23] of TMR versus bias were observed.

Nitrogen doping.—Recently it has been reported that nitrogen can be doped into MgO [24] as substitutional atoms to oxygen. Since OV causes a dramatic reduction of TMR, filling the OV with nitrogen may partially solve the problem. We have investigated this possibility and Fig. 2(d) plots the calculated TMR versus nitrogen concentration: TMR remains above 8000% when 4% of interfacial oxygen atoms are randomly replaced by nitrogen. This means diffusive scattering of spin-down electrons injected from Fe is much less effective by nitrogen impurity than by OV. Therefore, if viable experimental methods can be found to fill the almost unavoidable OVs near the Fe/MgO interface, it is possible to reach extremely high TMR ratio.

In summary, a few percent of interfacial OVs in MgO tunnel barrier is predicted to drastically reduce TMR ratio from the ideal theoretical limit to the presently observed experimental range. The physics is due to a very efficient diffusive scattering of spin-down channels in the Fe to the slowly decaying Δ_1 band of the MgO that reduces the coherent spin filtering effect. The application of the vertex correction theory [15] is important to capture this physics. Interior OV breaks the Δ_1 symmetry of the MgO barrier and significantly increases the junction resistance. The OV problem can be rectified by filling them with nitrogen atoms.

H. G. thanks Dr. S. S. P. Parkin for bringing the nitrogen doped MgO to our attention. We gratefully acknowledge financial support from NSERC of Canada, FQRNT of Quebec, and CIFAR (H. G.). K. X. is supported by NSF-China (10634070) and MOST (2011CB921803) of China. We thank RQCHP for computation facility.

[1] S. A. Wolf *et al.*, Science **294**, 1488 (2001).
[2] S. S. P. Parkin *et al.*, Nature Mater. **3**, 862 (2004).
[3] S. Yuasa *et al.*, Nature Mater. **3**, 868 (2004).
[4] S. Ikeda *et al.*, Appl. Phys. Lett. **93**, 082508 (2008).
[5] W. H. Butler, X.-G. Zhang, T. C. Schulthess, and J. M. MacLaren, Phys. Rev. B **63**, 054416 (2001).
[6] J. Mathon and A. Umerski, Phys. Rev. B **63**, 220403 (2001).
[7] X.-G. Zhang, W. H. Butler, and A. Bandyopadhyay, Phys. Rev. B **68**, 092402 (2003).
[8] D. Waldron, V. Timoshevskii, Y. Hu, K. Xia, and H. Guo, Phys. Rev. Lett. **97**, 226802 (2006).
[9] H. L. Meyerheim *et al.*, Phys. Rev. Lett. **87**, 076102 (2001); S. G. Wang *et al.*, J. Magn. Magn. Mater. **310**, 1935 (2007).
[10] M. Sicot *et al.*, J. Appl. Phys. **99**, 08D301 (2006); K. Miyokawa *et al.*, Jpn. J. Appl. Phys. **44**, L9 (2005); L. Plucinski, Y. Zhao, B. Sinkovic, and E. Vescovo, Phys. Rev. B **75**, 214411 (2007); P. Luches *et al.*, Surf. Sci. **583**, 191 (2005).
[11] G. X. Miao *et al.*, Phys. Rev. Lett. **100**, 246803 (2008).
[12] P. G. Mather, J. C. Read, and R. A. Buhrman, Phys. Rev. B **73**, 205412 (2006).
[13] J. P. Velev, K. D. Belashchenko, S. S. Jaswal, and E. Y. Tsymbal, Appl. Phys. Lett. **90**, 072502 (2007).
[14] J. Taylor, H. Guo, and J. Wang, Phys. Rev. B **63**, 121104 (R) (2001); **63**, 245407 (2001).
[15] Y. Ke, K. Xia, and H. Guo, Phys. Rev. Lett. **100**, 166805 (2008).
[16] O. K. Andersen and O. Jepsen, Phys. Rev. Lett. **53**, 2571 (1984).
[17] I. Turek *et al.*, *Electronic Structure of the Disordered Alloys, Surfaces and Interfaces* (Kluwer, Boston, 1997).
[18] P. Soven, Phys. Rev. **156**, 809 (1967); B. Velický, S. Kirkpatrick, and H. Ehrenreich, Phys. Rev. **175**, 747 (1968).
[19] The atomic structure is the same as that of Ref. [5]. For Fe, the atomic sphere has radius 1.411 Å whose space fills the bcc lattice. Inside MgO, we take radius 1.354 Å for oxygen atoms and 0.960 Å for Mg atoms. Vacuum sphere of radius 0.673 Å is added at the center of the cube with 4 O atoms and 4 Mg atoms to fill the space. The calculated MgO band gap is 5.8 eV within local spin density approximation. At the Fe/MgO interface, two vacuum spheres are inserted exactly above the vacuum spheres inside the MgO with the same radius, and a vacuum sphere of radius 0.814 Å is added exactly above the Mg atom to fill the total volume. Positions of the interfacial vacuum spheres are arranged to minimize overlap.
[20] J. Carrasco, N. Lopez, and F. Illas, Phys. Rev. Lett. **93**, 225502 (2004).
[21] For all MTJs, a 100×100 k mesh is used to sample the transverse two-dimensional BZ for converging the equilibrium density matrix. A 200×200 k mesh is used to converge the nonequilibrium density matrix. A 400×400 k mesh is used to converge the transmission coefficients of all spin channels.
[22] We do not consider trapping Fe atoms into OV because of the blind adsorption effect. See, for example, B. D. Yu, Phys. Rev. B **71**, 193403 (2005).
[23] D. V. Dimitrov *et al.*, J. Appl. Phys. **105**, 113905 (2009).
[24] C. H. Yang, M. Samant, and S. Parkin, in Proceedings of the American Physical Society 2009 March Meeting (to be published), Vol. 22, p00004; M. Pesci *et al.*, J. Phys. Chem. C **114**, 1350 (2010).